

**Mercury nonstoichiometry of the $\text{Hg}_{1-x}\text{Ba}_2\text{CuO}_{4+\delta}$ superconductor and
the P(Hg)-P(O₂)-T phase diagram of the Hg-Ba-Cu-O system.**

V.A.Alyoshin^{*}, D.A.Mikhailova, E.B.Rudnyi, E.V.Antipov.

Department of Chemistry, Moscow State University, 119899, Moscow, Russia.

Abstract

The P(Hg)-P(O₂)-T phase diagram of the Hg-Ba-Cu-O system for the Ba: Cu=2: 1 ratio was experimentally studied and followed by means of the thermodynamic modeling. It was shown that the $\text{Hg}_{1-x}\text{Ba}_2\text{CuO}_{4+\delta}$ (Hg-1201) superconductor possesses a significant range of Hg-nonstoichiometry and exists in a certain P(Hg), P(O₂) and T range. Mercury nonstoichiometry of Hg-1201 was investigated in the $923 \leq T \leq 1095$ K; $2.0 \leq P(\text{Hg}) \leq 8.4$ atm; $0.09 \leq P(\text{O}_2) \leq 0.86$ atm ranges. It was found that the mercury content varies in the range of 0.80-0.94 under these conditions. The Gibbs energy of the Hg-1201 phase was estimated as a function of temperature and mercury concentration. The obtained results allow optimizing the synthesis conditions of Hg-1201 with a given Hg-content including preparation of the Hg-stoichiometric phase.

PACS: 74.72-h

Keywords: $\text{HgBa}_2\text{CuO}_{4+\delta}$ superconductor, Hg-Ba-Cu-O system, Hg-nonstoichiometry, thermodynamic assessment.

1. Introduction

The $\text{HgBa}_2\text{CuO}_{4+\delta}$ (Hg-1201) superconductor with $T_c = 97$ K, the first member of the $\text{HgBa}_2\text{Ca}_{n-1}\text{Cu}_n\text{O}_{2n+2+\delta}$ homologous series ($n = 1$), discovered in 1993 [1], still attracts

^{*} Corresponding author: E-mail: alyoshin@inorg.chem.msu.ru

attention due to its relatively simple crystal structure and high T_c . The Hg-containing family exhibits the record values of T_c up to 138 K for the third member of the series. The Hg-1201 superconductor is considered as a model phase to study the relationship between the crystal structure and superconducting properties.

The high T_c values are supposed to be due to a perfect structure arrangement of the superconducting CuO_2 layers in these compounds. The extra oxygen atoms related to nonstoichiometric index δ occupy the oxygen positions in the center of squares in the HgO_δ planes, and changing δ results in variation of a copper valence (V_{Cu}) and, consequently, T_c . For these reasons, the main efforts were directed to study the oxygen nonstoichiometry and its influence on superconducting properties [2 - 5]. The cupola-shaped dependence of T_c vs. formal copper valence (V_{Cu}) or hole concentration (p) correlates with those for other known copper-oxide superconductors. The maximum T_c corresponds to $V_{\text{Cu}} = 2.16$, determined from iodometric titration data [2, 5], and $p = 0.16$ per Cu atom indirectly derived from the results of thermoelectric power study [6, 7].

For the Hg-1201 phase with the stoichiometric cation composition $\text{HgBa}_2\text{CuO}_{4+\delta}$, the extra oxygen content has to be equal to $\delta = \frac{1}{2}(V_{\text{Cu}} - 2)$, but numerous Neutron Powder Diffraction (NPD) studies did not confirm this fact. These NPD results are in contradiction with each other, as it was shown in Refs. [5, 8]. For instance, the δ values for the Hg-1201 phase exhibiting maximal T_c values were found to be 0.06 [9], 0.07 [8], 0.12 [5], 0.18 [10] and even 0.22 [6]. Moreover, the authors of Refs. [11, 12] found that T_c close to optimal value is practically constant in the wide δ range (0.06 - 0.17). We can conclude that the relationship between δ , V_{Cu} and T_c in Hg-1201 may be more complicated than for the ideal model.

These discrepancies might be caused, for instance, by an uncontrolled disturbance of the cation stoichiometry, more likely, the mercury one. Mercury can partly escape from the solid phase to the free volume of an ampoule in the course of the synthesis. *Wagner et al* [13] were

the first who pointed out that the mercury content in Hg-1201 can be less than the stoichiometric one. At present time, there is a number of papers where mercury deficiency was revealed on powder samples [4, 5, 8, 14] and even on single crystals [15]. One can suppose that the mercury deficiency is accompanied by the removal of the $[\text{HgO}_2]^{2-}$ dumbbell from the Hg-1201 structure with the formation of mercury point defects in HgO_δ layers and oxygen in BaO layers. This supposition may be indirectly confirmed by unusual high thermal parameters of mercury and respective oxygen atoms found in numerous diffraction studies of Hg-1201. In this case, in order to preserve the formal copper valence close to the optimal carrier concentration, the oxygen content in the HgO_δ layers is to increase. For instance, the removal of 5% $[\text{HgO}_2]^{2-}$ dumbbells would lead to an increase of the oxygen content in the HgO_δ layers by 0.05, in total it would be $\delta = 0.05 + \frac{1}{2}(V_{\text{Cu}} - 2)$. It should be noted that such a difference between the δ -values determined from the NPD and iodometric data on the same Hg-1201 samples was found in [5].

Up to now there are some experimental data that the mercury content in Hg-1201 depends on the synthesis conditions. The EDS analysis revealed its variation in the range 0.92(4) – 1.02(5) (Ba/Cu=2/1), depending on the way of sample synthesis [14]. The samples quenched from 800°C into cold water contained 0.92(4) mercury, but the slowly cooled samples showed mercury content near the stoichiometric, 1.02(5). It was shown also that slow cooling down to 600°C under partial oxygen and mercury pressures being constant is favorable for obtaining the mercury stoichiometric sample [16].

Thus, we can conclude that the Hg-1201 phase has a certain Hg-homogeneity range, and the mercury concentration depends on temperature and partial oxygen and mercury pressures. Synthesis at relatively low temperature (600 - 650°C) [17, 18] or/and synthesis with an excess of HgO (about 10% at 800°C [19]) can lead to the synthesis of practically stoichiometric Hg-1201. In order to obtain Hg-1201 samples with the required cation composition we have to

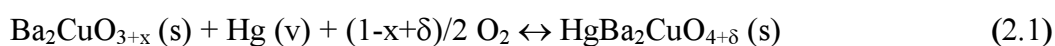
know the boundary of the Hg-1201 homogeneity region in the P(Hg)-P(O₂)-T coordinates and dependences of the Hg-concentration in Hg-1201 vs. temperature, P(Hg), and P(O₂). Up to now, there are no data describing the influence of these parameters on the Hg-content in the Hg-1201 phase. The phase diagram of the Hg-Ba-Cu-O system for the Ba/Cu = 2/1 ratio was computed in Ref [20] on the base of thermodynamic data without taking into account this problem.

The goals of the present work are to determine the dependences of the Hg-concentration in the Hg-1201 phase upon T, P(Hg) and P(O₂); to construct the P(Hg)-P(O₂)-T phase diagram of the Hg-Ba-Cu-O system for the Ba/Cu = 2/1 ratio from the result of simultaneous thermodynamic assesment; and finally, to optimize synthesis of Hg-1201 with the required cation stoichiometry.

2. Experimental

2.1. Sample preparation and characterization.

The synthesis of HgBa₂CuO_{4+δ} was carried out in a sealed silica tube from Ba₂CuO_{3+y} and mercury oxide. The initial reactions in sealed tubes occur mainly via vapor (v)/solid (s) interactions according to the following equilibria:



Pure HgO (99.9%), BaO₂ (99.99%), and CuO (99.99%) were taken as starting oxides. The Ba₂CuO_{3+y} precursor was obtained by annealing the fine mixture of BaO₂ and CuO taken in molar ratio 2/1 in oxygen flow at 900°C for 24h. The Hg-1201 phase was formed from pelletized Ba₂CuO_{3+x} and HgO mixtures taken in appropriate ratios. The alumina crucibles were used in order to prevent the interaction of precursor with silica tubes in which the experiments were carried out.

The redox pairs based on transition metals were used to adjust the partial oxygen pressure inside the closed silica tubes. The CoO/Co₃O₄ pair [21, 22] was used when P(O₂) < 1 atm:

$$\log P(\text{O}_2)[\text{atm}] = -15600/T + 12.6 \quad (1000-1240\text{K}), \quad (2.2)$$

whereas the Mn₂O₃/MnO₂ redox pair [21, 22] was used for higher pressures:

$$\log P(\text{O}_2)[\text{atm}] = -6890/T + 8.126 \quad (800-1000\text{K}). \quad (2.3)$$

The Hg-1201/Ba₂CuO_{3+x} pair was used to control the partial mercury pressure at fixed P(O₂).

The phase composition and lattice parameters were determined by X-ray powder diffraction (XRD) using Guinier-camera FR-552 (Cu-Kα₁ radiation, λ = 1.5406Å) with germanium as an internal standard. The titration by ammonium rhodanide was used for mercury content determination.

2.2. Static weight technique.

Two-temperature (Fig.1) and three-temperature (Fig.2) variations of the Static Weight Technique (SWT) were used in our investigations. The evacuated (10⁻² Torr) silica tubes of 19 cm length and 10 mm inner diameter loaded with substances were placed into a temperature-gradient furnace and suspended to an analytical balance. The accuracy of the ΔF (this value corresponds to the balance indication change) measurement was ±0.0005 g; the temperature inside the furnace was controlled with accuracy of ±2°C.

The two-temperature SWT was used by us earlier to study the three-phase *S*(Hg-1201)-*S*(Ba₂CuO_{3+x})-*V* equilibrium in the Hg-Ba-Cu-O system [16], while the three-temperature variation was applied in the present work. The two-temperature technique allows us to determine the mercury content in Hg-1201 and to calculate the mercury pressure over Hg-

1201 at fixed $P(O_2)$, while the three-temperature SWT allows us to determine the Hg-concentration in Hg-1201 at given $P(O_2)$ and $P(Hg)$.

For the calculation of partial pressures in these experiments, it was supposed that the silica tube is divided into two or three isothermal parts of known length (dashed lines in Figs.1, 2) with constant $P(Hg)$, $P(O_2)$, $P(HgO)$ inside each volume. The mass measurements after temperature change were done when balance indicator had stopped. This corresponds to achievement of steady state inside the ampoule volume, and the quasi-equilibrium states inside each isothermal volume. The equal values of the balance indicator for the measurements under heating and under cooling prove the achievements of these quasi-equilibrium states. Below we shortly describe the main principles, which were taken into account in the calculation.

2.2.1. Two-temperature static weight technique.

A mixture of known amounts of Ba_2CuO_{3+x} and HgO put at T_2 reacts under heating yielding Hg-1201 phase according to equation (2.1). Some amount of HgO evaporates into the ampoule volume with decomposition to Hg(v) and O_2 . It was supposed in our calculations that the extra oxygen index δ in Hg-1201 is equal to “x” in Ba_2CuO_{3+x} . A small amount of HgO(v) in vapor phase is present because of existence of the following equilibrium [21, 22]:



A part of oxygen is absorbed by CoO at T_1 (Fig.1) when $P(O_2)$ exceeds the oxygen pressure over the redox pair CoO/Co₃O₄, or eliminated from Co₃O₄ in the opposite case. Partial oxygen pressure at T_1 is described by equation (2.2) for the CoO/Co₃O₄ redox pair or by equation (2.3) for the Mn₂O₃/MnO₂ pair. Thus, we can write the following mass balance equation:

$$\Delta m_o(HgO/Ba_2CuO_{3+x}) = mV_1 + mV_2 + \Delta m_g(O_2) \quad (2.5)$$

$$\text{and } mV_i = m_i(O_2) + m_i(Hg) + m_i(HgO),$$

where mV_1 and mV_2 are vapor masses in volumes V_1 and V_2 , respectively; $m_i(O_2)$, $m_i(Hg)$, $m_i(HgO)$ are masses of O_2 , Hg , HgO in vapor in each volume V_i ; $\Delta m_o(HgO/Ba_2CuO_{3+x})$ is mass loss of the starting mixture; $\Delta m_g(O_2)$ is mass change of the oxygen getter (positive for absorption).

In this case the balance indication ΔF (Fig. 1) changes are as follows:

$$\Delta F = (mV_1 \cdot L_1 + mV_2 \cdot L_2 + \Delta m_g(O_2) \cdot L_3) / L_o \quad (2.6)$$

where L_o is length of the balance shoulder; L_1 , L_2 are distances between mass centers of a Hg-1201 pellet and volumes V_1 and V_2 ; L_3 is a distance between the mass centers of Hg-1201 and oxygen getter pellets.

The equation of mass balance of mercury and oxygen is:

$$\begin{aligned} m_1(O_2) + m_1(O_2)_{(HgO(v))} + m_2(O_2) + m_2(O_2)_{(HgO(v))} + \Delta m_g(O_2) = \\ = (m_1(Hg) + m_1(Hg)_{(HgO(v))} + m_2(Hg) + m_2(Hg)_{(HgO(v))}) \times M(O_2) / M(Hg) \end{aligned} \quad (2.7)$$

where $m_i(O_2)_{(HgO(v))}$, $m_i(Hg)_{(HgO(v))}$ are masses of oxygen and mercury in $HgO(v)$ molecules in isothermal volumes, respectively; $M(O_2)$, $M(Hg)$ are molar masses of O_2 and Hg , respectively.

The steady state without mass transfer corresponds to an absence of a gradient of the total pressure. Therefore, we can write down the next equation:

$$P_1(Hg) + P_1(O_2) + P_1(HgO) = P_2(Hg) + P_2(O_2) + P_2(HgO), \quad (2.8)$$

where P_i are vapor partial pressures in respective isothermal volumes. The partial pressures are related to vapor masses according to the ideal gas law.

$P(HgO)$ decreases when the temperature increases (2.4) and:

$$\Delta P(HgO) = \Delta P(Hg) + \Delta P(O_2), \quad (2.9)$$

where ΔP_i is the difference of the respective partial pressures at T_1 and T_2 .

The differences of partial pressures at T_1 and T_2 cause the mass transfer of HgO molecules from low T_2 to hot T_1 temperature with their decomposition at T_1 to Hg and O_2 , which then move in opposite direction. In the steady state, the mass flux of HgO is equal to

sum of the Hg and O₂ mass fluxes. In the case of the molecular diffusion of Hg and O₂ we can write, supposing that coefficients of the Hg and O₂ diffusion are equal, that:

$$\Delta P(\text{Hg}) = 2\Delta P(\text{O}_2) \quad (2.10)$$

since the O₂ molar flux (J_{O_2}) is equal to one half of the Hg flux (J_{Hg}) in accordance with the reaction (2.4).

The mercury concentration ($I-x$) in the single-phase Hg-1201 sample was calculated from the following equation:

$$I-x = (\text{mHg}_{(\text{HgO}(\text{start}))} - \text{mHg}(\text{v}) - \text{MHg}_{(\text{HgO}(\text{v}))})/\text{mHg}_{(\text{Hg-1201})} \quad (2.11)$$

where $\text{mHg}_{(\text{HgO}(\text{start}))}$ is mercury mass in the starting HgO + Ba₂CuO_{3+x} mixture; $\text{mHg}(\text{v})$ is mercury vapor mass; $\text{MHg}_{(\text{HgO}(\text{v}))}$ is mercury mass in HgO(v); $\text{mHg}_{(\text{Hg-1201})}$ is the calculated mass in stoichiometric Hg-1201.

Solving the system of equations (2.2)-(2.11) allows us to calculate P(Hg), P(HgO), P(O₂) at T₁ and T₂, and the mercury concentration in Hg-1201. These equations are applied for two-phase equilibrium $S(\text{Hg-1201})-V$ only.

2.2.2. Three-temperature static weight technique.

The scheme of the three-temperature SWT is shown in Fig.2. This technique is very close to the two-temperature one. The additional pellet of the Hg-1201 and Ba₂CuO_{3+x} mixture is placed in the central part of the tube to control P(Hg) in the tube for a fixed P(O₂). The main differences are described below. The balance indication ΔF , according to Fig.2, is determined as follows:

$$\Delta F = (\text{mV}_1 \cdot L_1 + \text{mV}_2 \cdot L_2 - \text{mV}_3 \cdot L_3 + \Delta \text{m}_g(\text{O}_2) \cdot L_4 + \Delta \text{m}(\text{Hg1201}) \cdot L_5)/L_0 \quad (2.12)$$

where mV_1 , mV_2 , mV_3 are vapor masses of V₁, V₂, V₃ volumes; $\Delta \text{m}(\text{Hg-1201})$ is mass change of the Hg-1201 sample at T₃; $\Delta \text{m}_g(\text{O}_2)$ is mass change of the oxygen getter; L₁ - L₅ are the distances between the respective mass centers as they are shown in Fig.2.

Mass balance equation (2.5) is changed in the following way:

$$\Delta m_o(\text{Hg-1201/Ba}_2\text{CuO}_{3+x}) = mV_1 + mV_2 + mV_3 + \Delta m_g(\text{O}_2) + \Delta m(\text{Hg-1201}) \quad (2.13)$$

where: $\Delta m_o(\text{Hg-1201/Ba}_2\text{CuO}_{3+x})$ - mass change of the Hg-1201/Ba₂CuO_{3+x} mixture at T₂.

2.2.3. Testing of SWT.

In order to check the correctness of the models used for the vapor pressure calculation from the SWT data and to estimate the precision of the results obtained, the following tests were performed.

Mercury oxide ($m(\text{HgO}) = 0.1121 \text{ g}$) was placed without oxygen getter in a silica tube at T₂ instead of Hg-1201 and heated, as in the two-temperature SWT (Fig.1). Temperatures T₁ and T₂ were varied independently in the 600-900°C (T₁) and 650-800°C (T₂) ranges for the unsaturated vapor. Deviation of the vapor mass, calculated from SWT data, from the starting $m(\text{HgO})$ did not exceed $\pm 2\%$ in these ranges (the total vapor pressure was about 4-6 atm). The same test with liquid mercury carried out in the temperature range 246-483°C ($0.075 < P(\text{Hg}) < 6.5 \text{ atm}$) showed that the difference between the measured saturated pressure and literature data [23] did not exceed $\pm 2\%$ also for $P(\text{Hg}) \geq 2 \text{ atm}$.

2.3. Annealing under controlled mercury and oxygen partial pressures.

Two variants of annealing under controlled mercury and oxygen pressures were used for the study of the Hg-Ba-Cu-O system in addition to SWT: polythermal (Fig.3, position (a)) and two-temperature (Fig.3, position (b)). In polythermal annealing the transition metal oxide mixture at highest temperature and pure HgO at lowest temperature are used to control P(O₂) and P(Hg) (at constant P(O₂)), respectively. Up to five Hg-1201 samples heated at different temperatures were used to determine the upper boundary of the Hg-1201 stability field.

In the two-temperature variant, pure HgO is used to control partial pressures of Hg and O₂, where their ratio 2/1 was suggested. We have neglected the difference in the oxygen stoichiometry in Hg-1201 and Ba₂CuO_{3+x}, because the values of extra oxygen content are

close to each other and experiments are carried out in large ampoules with a small amount of studied sample.

3. Results and discussion.

3.1. The $P(\text{Hg})$ - $P(\text{O}_2)$ - T phase diagram.

Two different phase equilibria of Hg-1201 with vapor and coexisting phases were studied in the Hg-Ba-Cu-O system: the three-phase equilibrium $S(\text{Hg-1201})$ - $S(\text{Ba}_2\text{CuO}_{3+x})$ - V and the four-phase equilibrium $S(\text{Hg-1201})$ - $S(\text{Ba}_2\text{Cu}_3\text{O}_{5+x})$ - $S(\text{BaHgO}_2)$ - V .

3.1.1. The $S(\text{Hg-1201})$ - $S(\text{Ba}_2\text{CuO}_{3+x})$ - V equilibrium.

This equilibrium corresponding to the reaction (2.1) describes the lower boundary of the Hg-1201 stability region. The dependence of the partial mercury pressure vs. $P(\text{O}_2)$ and T was studied earlier [16] using the two-temperature SWT. The experimental pressure values obtained in [20] agree well with this dependence. New experimental data were obtained for the higher oxygen pressure. The $\text{Mn}_2\text{O}_3/\text{MnO}_2$ getter was used to achieve the oxygen pressure up to 2.6 atm. A part of the new results obtained at 1.2 atm and literature data are presented in Fig.4 as temperature dependences of the mercury pressure at constant $P(\text{O}_2)$.

The following dependence was computed from all experimental data for $0.1 < P(\text{O}_2) < 2.6$ atm, $1.4 < P(\text{Hg}) < 6.5$ atm and $1009 < T < 1151$ K ranges:

$$\begin{aligned} \log P(\text{Hg})[\text{atm}] = & - (6514 \pm 178)/T - (0.329 \pm 0.010) \cdot \log(P\text{O}_2)[\text{atm}] + \\ & + (6.347 \pm 0.163), \end{aligned} \quad (3.1)$$

standard deviation (SD) = 0.024, number of points (N) = 50.

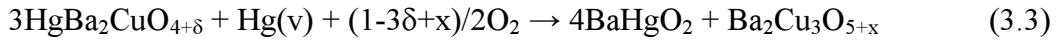
Therefore, the lower boundary of the Hg-1201 stability field as a function of $P(\text{Hg})$, $P(\text{O}_2)$, and T in the above quoted ranges is described as follows:

$$\log P(\text{Hg}) + 0.329 \log P(\text{O}_2) + 6514/T > 6.347. \quad (3.2.)$$

3.1.2. The $S(\text{Hg-1201})$ - $S(\text{Ba}_2\text{Cu}_3\text{O}_{5+x})$ - $S(\text{BaHgO}_2)$ - V equilibrium.

The upper boundary of the Hg-1201 stability field was deduced from the results of two-temperature and polythermal annealing of the samples heated at different $P(\text{O}_2)$ and $P(\text{Hg})$ for about 20-24 *h* followed by XRD analysis (Fig.4), and from the SWT data. Selected experimental results illustrating the influence of these parameters on the decomposition reaction are listed in Table 1.

These experiments showed that Hg-1201 decomposed at certain experimental conditions according to following reaction:



Therefore, we conclude that the four-phase equilibrium $S(\text{Hg-1201})$ - $S(\text{Ba}_2\text{Cu}_3\text{O}_{5+x})$ - $S(\text{BaHgO}_2)$ - V determines the upper boundary of the Hg-1201 stability field. K_p of the decomposition reaction (3.3) is expressed by the following equation:

$$K_p = P(\text{Hg})^{-1} \times P(\text{O}_2)^{-(1-3\delta+x)/2}.$$

We assumed that the oxygen coefficient $(1-3\delta+x)/2$ is equal to 0.75, because the extra oxygen content δ in Hg-1201 is close to 0.05, while x in $\text{Ba}_2\text{Cu}_3\text{O}_{5+x}$ is close to 0.65 [24] at these experimental conditions.

We could use only 7 experimental points, marked by asterisks in Tab.1 for the estimation of the numerical coefficients for the $P(\text{Hg})$ vs. $P(\text{O}_2)$ and T dependence. The selected experimental data correspond to the four-phase equilibrium, or their parameters (partial pressures and temperature) are close to the surface describing this equilibrium. The following expression describes this four-phase equilibrium:

$$\log P(\text{Hg})[\text{atm}] = -9851/T - 0.75 \cdot \log P(\text{O}_2)[\text{atm}] + 10.60 \quad (3.4)$$

$$(0.43 \leq P(\text{O}_2) \leq 4.7 \text{ atm}, 3.0 \leq P(\text{Hg}) \leq 10.3 \text{ atm}, 968 \leq T \leq 1073 \text{ K}, N = 7).$$

Therefore, the upper boundary of the Hg-1201 stability field is expressed by the equation:

$$\log P(\text{Hg}) + 0.75 \cdot \log P(\text{O}_2) + 9851/T < 10.60 \quad (3.5)$$

3.1.3. The P(Hg)-P(O₂)-T phase diagram.

The part of the 3-D P(Hg)-P(O₂)-T phase diagram of the Hg-Ba-Cu-O system for the cation ratio Ba/Cu = 2/1 shown in Fig. 5 was constructed using the results described above. The studied equilibria $S(\text{Hg-1201})-S(\text{Ba}_2\text{CuO}_{3+x})-V$ and $S(\text{Hg-1201})-S(\text{BaHgO}_2)-S(\text{Ba}_2\text{Cu}_3\text{O}_{5+x})-V$ are shown in this diagram as the surfaces sandwiching the Hg-1201 stability field. Ba₂CuO_{3+x} is stable below the lower surface, while BaHgO₂ and Ba₂Cu₃O_{5+x} are formed above the upper surface. As one can see, the region of the Hg-1201 stability field becomes larger with increasing T and decreasing P(O₂). This might be explained by the thermodynamical instability of Ba₂Cu₃O_{5+x} at low oxygen pressure and high temperature [24].

3.2. Mercury nonstoichiometry of Hg-1201.

The variation of mercury concentration in Hg-1201 vs. P(Hg), P(O₂), and T inside the stability field of the Hg-1201 phase was studied by the two- and three-temperature variants of SWT.

Two-temperature SWT study. The dependences of the mercury vapor pressure over Hg-1201 vs. T at P(O₂) = 0.4 atm for the experiments #F1 and #F2 are presented in Fig.6 and Tab.2. One can see from these experiments that the Hg_{1-x}Ba₂CuO_{4+δ} phase loses mercury under heating into the free volume of the ampoule with increasing the Hg-vapor pressure and decreasing the mercury concentration in the Hg-1201 phase until the three-phase equilibrium $S(\text{Hg-1201})-S(\text{Ba}_2\text{CuO}_{3+x})-V$ is achieved. Then the slope of the curve becomes much larger in according with this equilibrium. For comparison, we plotted by dashed lines the variation of P(Hg) vs. T if the Hg-1201 phase did not change its Hg-concentration under heating. Thus, we can conclude that the Hg-concentration in Hg-1201 changes inside the stability field of this phase.

Three-temperature SWT study. This technique was used in a wide range of parameters and Hg-concentration variation because the temperature of the sample and partial pressures, $P(\text{Hg})$, $P(\text{O}_2)$, can be changed independently in these experiments. Four different samples were used in these investigations, #F3 - #F6 (Tab.3). In all cases, except sample #F3, single-phase Hg-1201 samples were found after finishing the experiments and quenching the samples into cold water. The experiment #F3 differs from others because the last point lies outside the stability field of Hg-1201. This point corresponds to existence of BaHgO_2 and $\text{Ba}_2\text{Cu}_3\text{O}_{5+x}$ according to expression (3.5) describing the upper stability field of Hg-1201.

The variation of Hg-concentration vs. experimental conditions is given in Tab.3 together with the results of the rhodanometric determination of the mercury content. The discrepancies between the SWT data and the rhodanometric titration results of the single-phase solid samples did not exceed 2 at.% Hg.

By simultaneous treatment of all experimental data (Tabs.2 and 3) we were able to deduce the dependence of Hg-concentration ($I-x$) in the Hg-1201 phase vs. $P(\text{Hg})$, $P(\text{O}_2)$, and T by the following expression:

$$\begin{aligned} \log(I-x) = & 336.9(\pm 23.2)/T + 0.0657(\pm 0.0090) \times \log P(\text{Hg}) + \\ & + 0.0329(\pm 0.0045) \times \log P(\text{O}_2) - 0.419(\pm 0.023) \end{aligned} \quad (3.6)$$

in the $923 \leq T \leq 1095 \text{ K}$, $2.0 \leq P(\text{Hg}) \leq 8.4 \text{ atm}$, and $0.09 \leq P(\text{O}_2) \leq 0.86 \text{ atm}$ ranges,

$$\text{SD} = 0.0074, \text{ N} = 59$$

3.3. Thermodynamic assessment.

The experimental results described above have been combined with thermodynamical data available in literature to derive the Gibbs energies of all phases under equilibrium in the Hg-Ba-Cu-O system. The ratio $\text{Ba}/\text{Cu}=2/1$ as in the Hg-1201 phase has been fixed in the present modeling.

This computation was based on the thermodynamic properties of compounds listed in Tab. 4. The molar Gibbs energy computed from the coefficients shown in Tab. 4 is related to the "Standard Element Reference (SER)". The conception of the SER is discussed elsewhere, for example in Ref. [25].

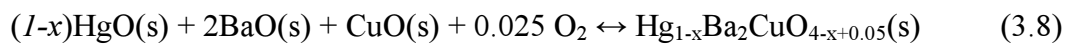
In order to describe the phase equilibria with the $\text{Hg}_{1-x}\text{Ba}_2\text{CuO}_{4+\delta}$ phase, it is necessary to employ the Gibbs energies of the coexisting phases. The Gibbs energies of the phases in the Ba-Cu-O system were used as given in Ref. [24] (see Tab. 5). The unknown Gibbs energy of the Hg-1201 phase depending on the mercury and oxygen composition and temperature was assessed from the experimental data and reference thermodynamical values (see Tab.6).

In order to compute the molar Gibbs energy of the $\text{Hg}_{1-x}\text{Ba}_2\text{CuO}_{4+\delta}$ phase, the extra oxygen index δ was assumed to be constant and equal to 0.05. This is a rather rough assumption, and the main reason behind it is the lack of a reliable experimental data set to estimate the Gibbs energy dependence vs. δ and T. As a result of this assumption, a known dependence of $\Delta_f H^\circ_{298}$ vs. δ , obtained from the calorimetric study [26], has not been used in the present work.

The mercury non-stoichiometry was modeled by means of the simple point-defect model where the molar Gibbs energy could be expressed as:

$$\Delta_{\text{ox}}G(T, x) = x g_1(T) + (1-x)g_2(T) + x(1-x)a_o(T) + RT[x \ln x + (1-x) \ln (1-x)] \quad (3.7)$$

where $g_i(T)$ and $a_o(T)$ are the temperature functions to be determined; $\Delta_{\text{ox}}G(T, x)$ – the Gibbs energy of formation from the oxides, HgO, BaO, CuO, and oxygen *i.e.*, the Gibbs energy of the reaction:

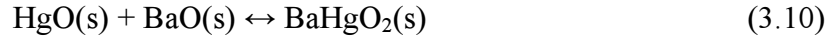


Therefore, the assessment of $\text{Hg}_{1-x}\text{Ba}_2\text{CuO}_{4+\delta}$ thermodynamics is equivalent to determining the unknown temperature functions, $g_i(T)$ and $a_o(T)$ Eq.(3.7). The latter determination is possible if we choose a certain analytical function of temperature and put

unknown parameters within it. In this way, the temperature dependence of these coefficients $g_i(T)$ and $a_o(T)$ and the Gibbs energy $G(T)$ by the same function was chosen as follows

$$(G(T), g_i(T), a_o(T)) = A + B T + C T \ln T + D T^{0.5} + E T^{-1} \quad (3.9)$$

The Gibbs energy of BaHgO₂ was also considered as an unknown function and it was determined in the present work simultaneously with the Gibbs energy of Hg_{1-x}Ba₂CuO_{4+δ} by means of modeling the Gibbs energy of the reaction



by Eq. (3.9) with its own unknown parameters.

The enthalpies, entropies and the heat capacities of reactions (3.8) and (3.10) are found from the Gibbs energies as

$$\Delta_{\text{ox}}H^{\text{calc}} = -T^2 \{ [\partial \Delta_{\text{ox}}G/T] / \partial T \} \quad (3.11)$$

$$\Delta_{\text{ox}}S^{\text{calc}} = -\{ \partial \Delta_{\text{ox}}G / \partial T \} \quad (3.12)$$

$$\Delta_{\text{ox}}C_p^{\text{calc}} = -T \{ \partial^2 \Delta_{\text{ox}}G / \partial T^2 \} \quad (3.13)$$

Table 6 lists the chosen experiments that have been used to determine the Gibbs energies of Hg_{1-x}Ba₂CuO_{4+δ} and BaHgO₂. A label was assigned to each experiment and all the data displayed are referred to this label.

The main principles of thermodynamic assessment are presented, for instance, in Ref. [24]. In the general form the relationship between the measured property and the controlled variables can be expressed as

$$y_{ij} = y_{ij}^{\text{calc}} \{ \mathbf{x}_{ij}; \Theta \} + \varepsilon_{ij} \quad (3.14)$$

where y_{ij}^{calc} is the value that is calculated by thermodynamical laws and differs from the experimentally measured y_{ij} by the experimental error ε_{ij} ; Θ is the vector of unknown

parameters to be determined (the unknowns in the Gibbs energies of $\text{Hg}_{1-x}\text{Ba}_2\text{CuO}_{4+\delta}$ and BaHgO_2).

As such, the formal task of the thermodynamic assessment could be expressed as follows. For the given experimental points $\{y_{ij}, x_i\}$, it is necessary to determine such parameters in the Gibbs energies, which give us the best description of the original experimental values.

In order to achieve the goal set above, the total experimental error was modeled by the linear error model [27], and the maximum likelihood method has been used to estimate unknown parameters in the Gibbs energies. The procedure in more details is described in [27], where there is also a comparison with the conventional least-squares method. The computations have been performed with the TDLIB software, available on the Internet at the address <http://www.chem.msu.su/~rudnyi/tllib/>.

We were able to describe the results of the phase equilibria experiments within the three standard deviations of the reproducibility (Fig.7). This supports our assumption that within the working conditions the oxygen index in the $\text{Hg}_{1-x}\text{Ba}_2\text{CuO}_{4+\delta}$ phase was roughly constant. The absolute standard deviations of calculated variable components are presented in Tab 7.

There is a good accordance of enthalpies of formation and specific heats of $\text{Hg}_{1-x}\text{Ba}_2\text{CuO}_{4+0.05}$ and BaHgO_2 with literature data. The discrepancy between the calculated and reference standard entropies of Hg-1201 is within $13 \text{ J}\cdot\text{K}^{-1}\cdot\text{mol}^{-1}$. We could note that the reference entropy was estimated with high error.

The standard deviation in mercury pressure in the three-phase equilibrium $S(\text{Hg-1201})-S(\text{Ba}_2\text{CuO}_{3+x})-V$ did not exceed 0.175 atm , the accuracy of mercury content determination was within 0.01. As for the four-phase equilibrium $S(\text{Hg-1201})-S(\text{BaHgO}_2)-S(\text{Ba}_2\text{Cu}_3\text{O}_{5+x})-V$, the agreement with mercury pressure determination was found to be within 0.8 atm despite of an interpolation method used for an estimation of the partial pressure of mercury. The reason

can be in limited number of experimental data for the determination of the Hg dependence in this equilibrium.

The computed coefficients for the $\text{Hg}_{1-x}\text{Ba}_2\text{CuO}_{4-x+0.05}$ and BaHgO_2 Gibbs energies are given in Tables 8 and 9. For comparison, the Gibbs energy of BaHgO_2 evaluated from Ref. [33] is put in Tab.9, which practically coincides with one assessed in this work.

This kind of agreement could be considered as satisfactory in our case. The problem here is that the simultaneous assessment of the Gibbs energies of $\text{Hg}_{1-x}\text{Ba}_2\text{CuO}_{4+\delta}$ and BaHgO_2 was performed in the present work while the Gibbs energies of barium cuprates from Ref. [24] were fixed. Provided the Gibbs energies of barium cuprates were assessed seven years ago from contradicting literature values, the overall agreement obtained in the present assessment, actually, could be named as even remarkable. In a way, the results obtained in present study confirm the reliability of the barium cuprates thermodynamics taken from Ref. [24].

3.4. $P(\text{Hg})$ - $P(\text{O}_2)$ and $P(\text{Hg})$ - T cross-section of the $P(\text{Hg})$ - $P(\text{O}_2)$ - T phase diagram and Hg-nonstoichiometry of $\text{Hg}_{1-x}\text{Ba}_2\text{CuO}_{4+\delta}$

The obtained thermodynamic functions were used for the computation of the $P(\text{Hg})$ - $P(\text{O}_2)$ at $T = \text{const}$ (Fig.8) and $P(\text{Hg})$ - T at $P(\text{O}_2) = \text{const}$ (Fig.9) cross-sections of the $P(\text{Hg})$ - $P(\text{O}_2)$ - T phase diagram of the Hg-Ba-Cu-O system. The available experimental results were plotted in these cross-sections also. We can conclude from the comparison of the experimental data and the results of calculation that the thermodynamic data presented in Tabs.4 - 6 allow to perform the thermodynamic assessment in spite of the approximations, which were made under calculation.

The $P(\text{Hg})$ - $P(\text{O}_2)$ cross-section at $T = 800^\circ\text{C}$ (Fig.8) is analogous in topology to the one computed in Ref. [20]. However, there are significant quantitative differences. The main

reasons for that are: 1) the description of the Hg-1201 phase as the Hg-nonstoichiometric compound with a variable Hg-concentration inside stability field was introduced, and 2) different approaches and data were used for the computation.

For instance, the computed in Ref. [20] inclination tangent of the three-phase equilibrium $S(\text{Hg-1201})-S(\text{Ba}_2\text{CuO}_{3+x})-V$ line ($\log P(\text{Hg})-\log P(\text{O}_2)$ coordinates) is larger than the experimental one (0.33(1) from Eq.3.1). The large slope equal to 0.5 was used in Ref. [34] also. According to the model discussed, the smaller slope of the experimental line is due to changing mercury concentration in Hg-1201 and different extra oxygen content of Hg-1201 and $\text{Ba}_2\text{CuO}_{3+x}$. The appearance of $\text{Ba}_2\text{Cu}_3\text{O}_{5+x}$ and BaHgO_2 at high mercury pressure was computed in this work and confirmed experimentally in contrast to results given in Ref. [20], where the existence of BaHgO_2 and CuO was predicted in these conditions. This difference might be caused by the usage of the lower value of enthalpy of the BaHgO_2 formation ($\Delta_{\text{ox}}H^\circ = -41.3 \text{ kJ/mol}$) in Ref. [20] which significantly differs from those ones reported in [32] ($-59.6 \pm 2.4 \text{ kJ/mol}$) and [33] ($-63 \pm 14 \text{ kJ/mol}$).

Two points from Tab.1 (points #5 and #6) corresponding to different phase compositions at 800°C , presented in Fig.8, and point #1 (Tab.1) corresponding to the $S(\text{Hg-1201})-S(\text{BaHgO}_2)-S(\text{Ba}_2\text{Cu}_3\text{O}_{5+x})-V$ equilibrium, presented in Fig.9 show the correctness of the computed diagram. It is clearly seen that a small increase of partial mercury and oxygen pressure dramatically changes the phase composition of solid state from Hg-1201 to the mixture of BaHgO_2 and $\text{Ba}_2\text{Cu}_3\text{O}_{5+x}$.

Several important conclusions can be made from these data. First, the Hg-concentration in the Hg-1201 phase is lower than the stoichiometric value at commonly used synthesis conditions in sealed tube, and, therefore, the Hg-stoichiometric phase cannot be prepared by annealing under these conditions followed by rapid quenching. Moreover, the stoichiometric composition cannot be achieved at higher mercury pressure, as it is limited by pressure of

saturated vapor over liquid mercury (line Hg(liq.) in Fig.9) or over mercury oxide. Second, the stability field of Hg-1201 becomes narrow upon $P(O_2)$ increasing, and this fact explains why the formation of this phase is often suppressed when oxygen-rich starting mixtures (like peroxides or an excess of HgO) are directly used for the synthesis in closed vessels without special efforts to decrease internal oxygen pressure. But, on other hand, the higher oxygen pressure favors the increasing of the mercury content in Hg-1201.

It is important to notice that the Hg-1201 stability field becomes larger at higher temperature, or at lower partial oxygen pressure. Therefore, at low $P(O_2)$ an increase of $P(Hg)$ should result in an increase of Hg-concentration in Hg-1201 while at higher $P(O_2)$ it can lead to a decomposition of Hg-1201. We can estimate that nearly stoichiometric Hg-1201 phase can be obtained at relatively low oxygen pressure (about 0.1 atm) at $T = 800^\circ C$ if $P(Hg)$ exceeds 1000 atm. Such high mercury pressure cannot be achieved in conventional sealed tube synthesis, and, moreover, the vapor pressure over liquid mercury much lower (about 100 atm) at this temperature. However, a two-step procedure can help to overcome this problem and prepare nearly stoichiometric Hg-1201.

According to the $P(Hg)$ - T cross-section at $P(O_2) = 0.42$ atm (Fig.9), in order to obtain such sample, Hg-1201 with a low Hg-concentration should be synthesized in the phase stability region, then slowly cooled at constant mercury and oxygen pressures down to 600 - 650°C, and treated at this temperature for a short time to increase the Hg-concentration in Hg-1201.

The synthesis at 800°C of nearly Hg-stoichiometric 1201 phase was described in Ref. [16]. The Hg-concentration in the Hg-1201 phase can not exceed 84% according to Fig.9 if the sample was prepared at $P(O_2) = 0.42$ atm and $P(Hg) = 4.5$ atm (line AB, Fig.9). Then the sample was treated for several hours at lower temperature under the same Hg and O_2 partial pressures. This additional procedure resulted in an increase of the Hg-concentration up to the

value close to ideal one. For instance, the pure Hg-1201 sample quenched from 700°C (point *C* in Fig.9) has the Hg-content of 0.91(2), while the samples slowly cooled from 800°C to 650°C and treated about one hour at this temperature before quenching (point *D*) have the Hg-concentration equal to 0.96(2) according to rhodanometric titration. The calculated Hg-concentrations are close to the experimental ones and they are equal to 0.90(1) at 700°C and 0.94(1) at 650°C. The second treatment takes place at metastable conditions for Hg-1201, however, relatively low temperature prevents the decomposition reaction with formation of BaHgO₂ and Ba₂Cu₃O_{5+x}, or BaHgO₂ and CuO due to a kinetic reason. The longer annealing time (12 h), as it was shown in section 3.2, resulted in a decomposition of Hg-1201 according to the equilibrium phase diagram. It should be mentioned that slow cooling allows also to prepare the nearly-stoichiometric Hg-1201 phase (0.99(2) Hg) as it was described in Ref. [16].

Conclusion

The P(Hg)-P(O₂)-T phase diagram of the Hg-Ba-Cu-O system for the Ba/Cu=2/1 ratio was studied and followed by the thermodynamics modeling. Experimental vapor pressures in this system and literature thermodynamic data were used in the calculations. The calculated and experimental values are in good agreement. The Hg-1201 stability field is sandwiched between the surfaces of the $S(\text{Hg-1201})\text{-}S(\text{Ba}_2\text{CuO}_{3+x})\text{-}V$ and $S(\text{Hg-1201})\text{-}S(\text{BaHgO}_2)\text{-}S(\text{Ba}_2\text{Cu}_3\text{O}_{5+x})\text{-}V$ equilibria. It was shown that the Hg_{1-x}Ba₂CuO_{4+δ} (Hg-1201) superconductor possesses a significant range of the Hg-nonstoichiometry and exists in a certain P(Hg), P(O₂) and T range. The mercury nonstoichiometry of Hg-1201 was investigated in the $923 \leq T \leq 1095$ K; $2.0 \leq P(\text{Hg}) \leq 8.4$ atm; $0.09 \leq P(\text{O}_2) \leq 0.86$ atm ranges. It was found that the mercury content varies in the range of 0.80-0.94 under these conditions. The Gibbs energy of the Hg-1201 phase was calculated as a function of temperature and mercury concentration. The

obtained results allow optimizing the synthesis conditions of Hg-1201 and varying Hg-concentration including preparation of the Hg-stoichiometric phase.

Acknowledgments

This work was partly supported by Russian Foundation for Basic Research (00-03-32379), Russian Scientific Program on Superconductivity (Poisk), INTAS (99-1136) and Volkswagen Stiftung (I/75849). The authors are grateful to Dr. A.V.Shevelkov for valuable comments.

References.

- [1]. S.N. Putilin, E.V. Antipov, O. Chmaissem, M. Marezio. *Nature (London)* 362 (1993) 226.
- [2]. A. Fukuoka, A. Tokiwa-Yamamoto, M. Itoh, K. Usami, S. Adachi, H. Yamauchi, K. Tanabe. *Physica C* 265 (1996) 13.
- [3]. J.-F. Marucco, V. Vialett, A. Bertinotti, D. Colson, A. Forget. *Physica C* 275 (1997) 12.
- [4]. T. Tsuchiya, K. Fueki, T. Koyama. *Physica C* 298 (1998) 49.
- [5]. V.L. Aksenov, A.M. Balagurov, V.V. Sikolenko, V.G. Simkin, V.A. Alyoshin, E.V. Antipov, A.A. Gippius, D.A. Mikhailova, S.N. Putilin, F. Bouree. *Phys.Rev.B* 55 (1997) 3966.
- [6]. Q. Xiong, Y.Y. Xue, Y. Cao, F. Chen, Y.Y. Sun, J. Gibson, C.W. Chu, L.N. Liu, A. Jacobson. *Phys.Rev.B* 50 (1994) 10346.
- [7]. Q. Xiong, Y.Y. Xue, Y. Cao, F. Chen, J. Gibson, L.N. Liu, A. Jacobson, C.W. Chu. *Physica C* 251 (1995) 216.
- [8]. N.C. Hyatt, J.P. Hodges, I. Gameson, S. Hull, P.P. Edwards. *J. of Solid State Chemistry* 148 (1999) 119.
- [9]. O. Chmaissem, Q. Huang, S.N. Putilin, M. Marezio, A. Santoro. *Physica C*, 212 (1993) 259.
- [10]. Q. Huang, J.W. Lynn, Q. Xiong, C.W. Chu. *Phys. Rev. B* 52 (1995) 462.
- [11]. B. Dabrowski, J.L. Wagner, D.G. Hinks, J.F. Mitchell, J.D. Jorgensen, O. Chmaissem. *Physica B* 241 (1997) 805.
- [12]. J.D. Jorgensen, O. Chmaissem, J.L. Wagner, W.R. Jensen, B. Dabrowski, D.G. Hinks, J.F. Mitchell. *Physica C* 282-287 (1997) 97.
- [13]. J.L. Wagner, P.G. Radaelli, D.G. Hinks, J.D. Jorgensen, J.F. Mitchell, D. Dabrowski, G.S. Knapp, M.A. Beno. *Physica C* 210 (1993) 447.
- [14]. Y.Y. Xue, Q. Xiong, Y. Cao, I. Rusakova, Y.Y. Sun, C.W. Chu. *Physica C* 255 (1995) 1.
- [15]. P. Border, F. Duc, S. LeFloch, J.J. Capponi, E. Alexandre, M. Rosa-Nunes, S. Putilin, E.V. Antipov. *Physica C* 271 (1996) 189.
- [16]. V.A. Alyoshin, D.A. Mikhailova, E.V. Antipov. *Physica C* 271 (1996) 197.
- [17]. A. Yamamoto, M. Itoh, A. Fukuoka, S. Adachi, H. Yamauchi, K. Tanabe. *J. of Materials Research* 14 (1999) 644.
- [18]. Ayako Yamamoto, Wei-Zhu Hu, Setsuko Tajima. *Physica C* 335 (2000) 268.
- [19]. V.A. Alyoshin, D.A. Mikhailova, E.V. Antipov. *Physica C* 255 (1995) 173.

- [20]. D. Sedmidubský, J. Leitner, K. Knížek, A. Strejc, M. Veverka. *Physica C* 329 (2000) 191.
- [21]. I.S. Kulikov. *Termodinamika oksidov, Spravochnik* (Russian), Moskow (1986).
- [22]. JANAF International Tables, NBS USA, Washington, 1971 - 1975.
- [23]. A.N.Nesmeyanov. *Davlenie para khimicheskikh elementov* (Vapor pressure of chemical elements). Moscow, RAN, 1961, p.24 (Russian)
- [24]. G.F. Voronin, S.A. Degterev. *J.of Solid State Chemistry* 110 (1994) 50.
- [25]. A.T. Dinsdale. SGTE data for pure substances. *CALPHAD*, 1991, v. 15, N 4, p. 317.
- [26]. V.A. Alyoshin, D.A. Mikhailova, E.V. Antipov, A.S. Monaenkova, A.A. Popova, L.A.Tiphlova, J.Karpinski. *Journal of Alloys and Compounds* 284 (1999) 108.
- [27]. E.B. Rudnyi, V.V. Kuzmenko, G.F. Voronin. *J. Phys. Chem. Ref. Data* 27 (1998) 855.
- [28]. L.V. Gurvich, *High Temp. Sci.*, 1989, 26, 197. (IVTAN-THERMO)
- [29]. M.V. Gorbacheva, A.F. Maiorova, S.N. Mudretsova, E.B. Rudnyi, A.D. Rusin. M.V. *Zh. Fiz. Khim. (J. Phys. Chem.)* 72 (1998) 416 (in Russian).
- [30]. V.A. Aleshin, M.V. Gorbacheva, A.F. Maiorova, D.A. Mikhailova, S.N. Mudretsova, *Zh. Fiz. Khim. (J. Phys. Chem.)* 72 (1998) 421 (in Russian).
- [31]. M.V. Gorbacheva, A.F. Maiorova, S.N. Mudretsova. *Trudy Vserossiiskoi konferentsii po termicheskomu analizu*, Kazan, 1996, p. 138 (in Russian).
- [32]. A.S. Monaenkova, L.A. Tiphlova, A.A. Popova, A.V. Ignatov, V.A.Alyoshin. *Russ. J. Phys. Chem.* 75 (2001) 1246.
- [33]. D.A. Mikhailova, V.A. Alyoshin, E.V. Antipov, J. Karpinski. *J.Solid State Chemistry* 146 (1999) 151.
- [34]. T. Tsuchiya, K. Fueki, T. Koyama. *Physica C* 258 (1998) 49.

Figure captions

Fig.1. Scheme of the two-temperature static weight technique.

Fig.2. Scheme of the three-temperature static weight technique.

Fig.3. Schemes of the polythermal (a) and two-temperature (b) annealing experiments.

Fig.4. The dependences of $P(\text{Hg})$ vs. T at fixed $P(\text{O}_2)$ for the three-phase $S(\text{Hg}1201)$ - $S(\text{Ba}_2\text{CuO}_{3+y})$ - V equilibrium (1,2 - $\text{CoO}/\text{Co}_3\text{O}_4$ getter , 3 - $\text{Mn}_2\text{O}_3/\text{MnO}_2$ getter)

Fig.5. The $P(\text{Hg})$ - $P(\text{O}_2)$ - T phase diagram of the Hg-Ba-Cu-O system for the Ba/Cu=2/1 ratio

Fig.6. The $P(\text{Hg})$ vs. T dependences over Hg-1201 in the two-phase equilibrium $S(\text{Hg}-1201)$ - V (dashed lines – the calculated Hg-pressures if the Hg-concentration in Hg-1201 is constant).

Fig.7. Normalized deviates by the standard deviation, $\varepsilon_{ij}/\sigma_{r,i}$ for the experiments related to the phase equilibria. Labels of experimental points according to Tab.6.)

Fig.8. The computed $P(\text{Hg})$ - $P(\text{O}_2)$ cross-section of the $P(\text{Hg})$ - $P(\text{O}_2)$ - T phase diagram of the Hg-Ba-Cu-O system at $T = 800^\circ\text{C}$ for the Ba/Cu=2/1 ratio.

Dashed lines are the $(1-x)$ Hg-isoconcentrates inside the Hg-1201 homogeneity region. Diamonds show experimental points for the $S(\text{Hg}-1201)$ - $S(\text{Ba}_2\text{CuO}_{3+x})$ - V equilibrium at this temperature. Circles (filled and empty) represent the results from Tab.1 (\bullet - point #5, \circ - point #6).

Fig.9. The computed $P(\text{Hg})$ - T cross-section of the $P(\text{Hg})$ - $P(\text{O}_2)$ - T phase diagram of the Hg-Ba-Cu-O system at $P(\text{O}_2) = 0.42 \text{ atm}$ for the Ba/Cu=2/1 ratio.

Dashed lines are the $(1-x)$ Hg-isoconcentrates inside the Hg-1201 homogeneity region spread into a metastable region for a higher mercury pressure. Squares are the experimental points for the $S(\text{Hg}-1201)$ - $S(\text{Ba}_2\text{CuO}_{3+x})$ - V equilibrium from Fig.4 at this $P(\text{O}_2)$. Empty circle (\circ) represents the point #1 from Tab.1 corresponding to the $S(\text{Hg}-1201)$ - $S(\text{BaHgO}_2)$ - $S(\text{Ba}_2\text{Cu}_3\text{O}_{5+x})$ - V equilibrium.

Table 1.

Selected experiments illustrating the determination of the Hg-1201 upper boundary stability field.

No	T, °C	P(O ₂), atm	P(Hg), atm	Phase composition
Polythermal annealing				
1	840 760 743 730 *	0.43	10.3	Hg-1201 Hg-1201 Hg-1201 Hg-1201, BaHgO ₂ , Ba ₂ Cu ₃ O _{5+x}
Two-temperature annealing				
2	680	2.90	5.80	BaHgO ₂ , Ba ₂ Cu ₃ O _{5+x}
3	750	1.73	3.45	Hg-1201
4	750 *	2.46	4.92	BaHgO ₂ , Ba ₂ Cu ₃ O _{5+x}
5	800 *	4.06	8.12	Hg-1201
6	800 *	4.75	9.50	BaHgO ₂ , Ba ₂ Cu ₃ O _{5+x}
Static weight technique investigation				
7	695 *	0.66	3.28	Hg-1201
8	700 *	0.81	3.04	Hg-1201
9	700 *	1.36	3.27	Hg-1201, BaHgO ₂ , Ba ₂ Cu ₃ O _{5+x}

* - these values were used in calculations of the upper boundary of the Hg-1201 stability field.

Table 2.

The results of the two-temperature SWT investigation of the mercury nonstoichiometry of Hg_{1-x}Ba₂CuO_{4+δ}

T, °C	P(O ₂), atm	P(Hg), atm	Hg, (1-x)	T, °C	P(O ₂), atm	P(Hg), atm	Hg, (1-x)
Sample #F1				804	0.417	3.671	0.843
747	0.412	3.172	0.842	822	0.418	3.982	0.816
776	0.425	3.344	0.837	732	0.109	3.732	0.823
800	0.417	3.580	0.828	756	0.110	3.930	0.808
831	0.418	3.856	0.818	775	0.111	4.021	0.804
Sample #F2				786	0.112	4.136	0.795
763	0.412	3.486	0.853	750	0.093	3.762	0.824
771	0.413	3.495	0.853	751	0.204	3.731	0.827
776	0.414	3.552	0.849				

Table 3.

The results of the three-temperature SWT investigation of the mercury nonstoichiometry of $\text{Hg}_{1-x}\text{Ba}_2\text{CuO}_{4+\delta}$ ^{*)}

T, °C	P(O ₂), atm	P(Hg), atm	Hg, (1-x)	T, °C	P(O ₂), atm	P(Hg), atm	Hg, (1-x)
Sample #F3				Sample #F4			
750	0.405	4.559	0.861	750	0.413	2.952	0.845
770	0.408	4.772	0.850	770	0.413	3.564	0.836
730	0.404	4.072	0.871	790	0.411	4.778	0.835
730	0.666	3.984	0.876	730	0.413	2.491	0.853
702	0.664	3.434	0.876	730	0.676	2.642	0.865
695	0.664	3.279	0.881	755	0.676	3.152	0.866
700	0.811	3.043	0.878	754	0.187	3.807	0.859
740	0.666	4.214	0.869	770	0.189	4.431	0.855
740	0.186	4.225	0.859	790	0.189	5.431	0.852
761	0.187	4.583	0.852	710	0.676	2.705	0.866
680	0.666	2.850	0.886	730	0.679	1.998	0.863
700	0.664	3.395	0.881	730	0.860	2.687	0.877
^{#)} 700	1.361	3.269	-	750	0.863	2.725	0.872
				780	0.863	3.473	0.868
				Rhodanometric titration:			0.87(2)
Sample #F5				Sample #F6			
680	0.094	7.818	0.928	680	0.170	6.362	0.938
660	0.092	7.487	0.935	700	0.131	6.835	0.924
700	0.097	7.824	0.916	720	0.134	6.990	0.917
650	0.090	7.404	0.922	680	0.129	6.400	0.928
710	0.097	8.424	0.888	660	0.222	5.609	0.928
690	0.095	7.988	0.900	680	0.223	6.325	0.923
710	0.098	8.336	0.887	680	0.097	6.371	0.922
680	0.093	8.069	0.893	710	0.100	7.111	0.913
Rhodanometric titration:			0.88(2)	725	0.100	7.506	0.903
				680	0.170	6.256	0.922

^{#)} Phase composition (XRD data): 70% Hg-1201, 20% BaHgO₂, 10% Ba₂Cu₃O_{5+x}. Experiment was interrupted when mercury content in solid state was equal to 1.13 (1.11(2) from rhodanometric titration).

^{*)} The presented data are listed in sequence of the experiments carried out.

Table 4.

Auxiliary thermodynamic properties of key oxides and elements employed in the present work ^a

	A	B	C	D	E	F	Ref.
BaO(s)	-553092.97	463.41195	-72.028	-1858.564	0	-9963433	[27]
CuO(s)	-167369.13	477.64762	-69.785	-1801.184	61609	0	[27]
Hg(g) ^b	55196.294	-35.85579	-20.7537	0	-927.854	0	[28]
HgO(s)	-101735.10	361.28148	-60.23	-921.97	127811	0	[29]
O ₂ (g)	-1776.280	132.54252	-44.978	-1294.168	0	-13651002	[28]

^a the parameters allow us to compute $G^\circ - H^\circ_{\text{SER}}$ at standard pressure ($p^\circ = 101325$ Pa) according to the equation:

$$G^\circ - H^\circ_{\text{SER}} = A + B T + C T \ln T + D T^{0.5} + E T^{-1} + F T^{-2}$$

in $\text{J}\cdot\text{mol}^{-1}$ in the temperature interval from 250 K to 1300 K. A large number of significant digits in the parameters is given in order to overcome the strong correlation among them.

^b the equation $G^\circ - H^\circ_{\text{SER}} = A + B T + C T \ln T + D T^{0.5} + E T^{-1} + F T^{-2} + K T^2 + L T^3 + M T^4$ was used, where the additional coefficients are: $K = -2.76374\text{e-}05$, $L = 4.606922\text{e-}09$, $M = -3.434378\text{e-}13$

Table 5.

Auxiliary thermodynamic properties of reactions employed in the present work according to Ref. [24] ^a

Reaction	A	B	C
$2\text{CuO} - 0.5\text{O}_2 = \text{Cu}_2\text{O}$	145204.5	-190.334	11.9295
$\text{BaO} + 0.5\text{O}_2 = \text{BaO}_2$	-70889	65.102	0
$\text{BaO} + \text{Cu}_2\text{O} = \text{BaCu}_2\text{O}_2$	-46080	3.5170	0.3991
$\text{BaO} + \text{CuO} = \text{BaCuO}_2$	-38820	-3.2676	1.0975
$\text{BaO} + \text{CuO} + 0.05\text{O}_2 = \text{Ba}_2\text{CuO}_{3.1}$	-76243	24.860	0
$\text{BaO} + \text{CuO} + 0.15\text{O}_2 = \text{Ba}_2\text{CuO}_{3.3}$	-97187	42.902	0
$2\text{BaO} + 3\text{CuO} = \text{Ba}_2\text{Cu}_3\text{O}_5$ ^b	-49282	8.31441	0
$2\text{BaO} + 3\text{CuO} + 0.05\text{O}_2 = \text{Ba}_2\text{Cu}_3\text{O}_6$ ^b	-142980	83.8010	0

^a the parameters allow us to compute $\Delta_r G^\circ$ at standard pressure ($p^\circ = 101325$ Pa) according to the equation

$$\Delta_r G^\circ = A + B T + C T \ln T$$

in $\text{J}\cdot\text{mol}^{-1}$ in the temperature interval from 298 K to 1250 K

^b $\text{Ba}_2\text{Cu}_3\text{O}_5$ and $\text{Ba}_2\text{Cu}_3\text{O}_6$ are the end members of the binary solution $\text{Ba}_2\text{Cu}_3\text{O}_{5+x}$. The Gibbs energy of the mixture was described as

$$\Delta_{\text{mix}} G(T, x) = -73681.47x(1-x) + RT[x \ln x + (1-x) \ln (1-x)]$$

Table 6.

The experimental results taken into account in the assessment of the $\text{Hg}_{1-x}\text{Ba}_2\text{CuO}_{4+\delta}$ phase thermodynamics

Label	Set of values	N_I^{*j}	Comment	Reference
$\Delta_{\text{ox}}H^\circ$ (Hg-1201)	$\{\Delta_{\text{ox}}H_{ij}, T_{ij}\}$	1	$\text{HgBa}_2\text{CuO}_{4.05}$	[26]
S° (Hg-1201)	$\{S_{ij}, T_{ij}\}$	1	$\text{HgBa}_2\text{CuO}_{4.05}$	[30]
Cp° (Hg-1201)	$\{C_{p_{ij}}, T_{ij}\}$	21	$\text{HgBa}_2\text{CuO}_{4.05}$	[30]
Cp° (BaHgO_2)	$\{C_{p_{ij}}, T_{ij}\}$	5	BaHgO_2	[31]
$\Delta_{\text{ox}}H^\circ$ (BaHgO_2)	$\{\Delta_{\text{ox}}H_{ij}, T_{ij}\}$	1	BaHgO_2	[32]
Kp (BaHgO_2)	$\{K_{p_{ij}}, T_{ij}\}$	9	$\text{BaHgO}_2 = \text{BaO} + \text{Hg} + 0.5 \text{O}_2$	[33]
E1	$\{p(\text{Hg})_{ij}, T_{ij}, p(\text{O}_2)_{ij}\}$	10	$\text{Hg}_{1-x}\text{Ba}_2\text{CuO}_{4+\delta} + \text{Ba}_2\text{CuO}_{3+x} + \text{V}$	[16] + present work
E2	$\{p(\text{Hg})_{ij}, T_{ij}, p(\text{O}_2)_{ij}\}$	8		
E3	$\{p(\text{Hg})_{ij}, T_{ij}, p(\text{O}_2)_{ij}\}$	1		
E4	$\{p(\text{Hg})_{ij}, T_{ij}, p(\text{O}_2)_{ij}\}$	3		
E5	$\{p(\text{Hg})_{ij}, T_{ij}, p(\text{O}_2)_{ij}\}$	7		
E6	$\{p(\text{Hg})_{ij}, T_{ij}, p(\text{O}_2)_{ij}\}$	19		
E7	$\{p(\text{Hg})_{ij}, T_{ij}, p(\text{O}_2)_{ij}\}$	1		
E8	$\{p(\text{Hg})_{ij}, T_{ij}, p(\text{O}_2)_{ij}\}$	2		
F1	$\{x_{ij}, T_{ij}, p(\text{Hg})_{ij}, p(\text{O}_2)_{ij}\}$	3	$\text{Hg}_{1-x}\text{Ba}_2\text{CuO}_{4+\delta} + \text{V}$	Tab.2
F2	$\{x_{ij}, T_{ij}, p(\text{Hg})_{ij}, p(\text{O}_2)_{ij}\}$	11		
F3	$\{x_{ij}, T_{ij}, p(\text{Hg})_{ij}, p(\text{O}_2)_{ij}\}$	12	$\text{Hg}_{1-x}\text{Ba}_2\text{CuO}_{4+\delta} + \text{V}$	Tab.3
F4	$\{x_{ij}, T_{ij}, p(\text{Hg})_{ij}, p(\text{O}_2)_{ij}\}$	14		
F5	$\{x_{ij}, T_{ij}, p(\text{Hg})_{ij}, p(\text{O}_2)_{ij}\}$	8		
F6	$\{x_{ij}, T_{ij}, p(\text{Hg})_{ij}, p(\text{O}_2)_{ij}\}$	11		
G1	$\{p(\text{Hg})_{ij}, T_{ij}, p(\text{O}_2)_{ij}\}$	5	$\text{Hg}_{1-x}\text{Ba}_2\text{CuO}_{4+\delta} + \text{BaHgO}_2 + \text{Ba}_2\text{Cu}_3\text{O}_{5+x} + \text{V}$	From Tab.1

N_I^{*j} – number of experiments

Table 7.

Standard deviation of the variable components under the thermodynamic assessment of the phase equilibria in the Hg-Ba-Cu-O system.

Variable components	Standard deviation $\sqrt{\sigma_{r,i}^2}$
$\Delta_{\text{ox}}H^\circ$ (Hg-1201)	3.5 kJ·mol ⁻¹
S° (Hg-1201)	13 J·K ⁻¹ mol ⁻¹
C_p° (Hg-1201), C_p° (BaHgO ₂)	1.03 J·K ⁻¹ mol ⁻¹
$\Delta_{\text{ox}}H^\circ$ (BaHgO ₂)	1.74 kJ·mol ⁻¹
P(Hg) in three-phase equilibrium Hg _{1-x} Ba ₂ CuO _{4+δ} + Ba ₂ CuO _{3.3} + V (group of points E1-E8, tab.6)	0.175 atm
Mercury content in Hg-1201 (group of points F1-F6, tab.6)	0.0102
P(Hg) in four-phase equilibrium Hg _{1-x} Ba ₂ CuO _{4+δ} + BaHgO ₂ + Ba ₂ Cu ₃ O _{5+x} + V (group of points G1, tab.6)	0.78 atm

Table 8.

The parameters within Eq. (3.7) obtained for the Hg_{1-x}Ba₂CuO_{4-x+0.05} phase^a

	A	B	C	D	E
g_1	-31247	35.199	0	0	
g_2	-88855	494.18	-55.865	-3896.3	-1.1691e+05
a_0	-66006	0	0	0	

^a g_1 , g_2 , and a_0 are the temperature functions within Eq. (3.7), and A, B, C, D, E are the parameters within each temperature function according to the Eq. (3.9). The values given lead to the Gibbs energy in J·mol⁻¹. The Gibbs energy can be computed in the temperature range from 250 to 1250 K.

Table 9.

The parameters within Eq. (3.9) obtained for the formation of the BaHgO₂ phase according to reaction (3.10)

A	B	C	D	E	$\Delta_{\text{ox}}G^\circ_{298}$ kJ/mol	$\Delta_{\text{ox}}G^\circ_{298}$ kJ/mol [33]
-45219	300.41	-34.037	-2816.6	0	-62.1	-61.5

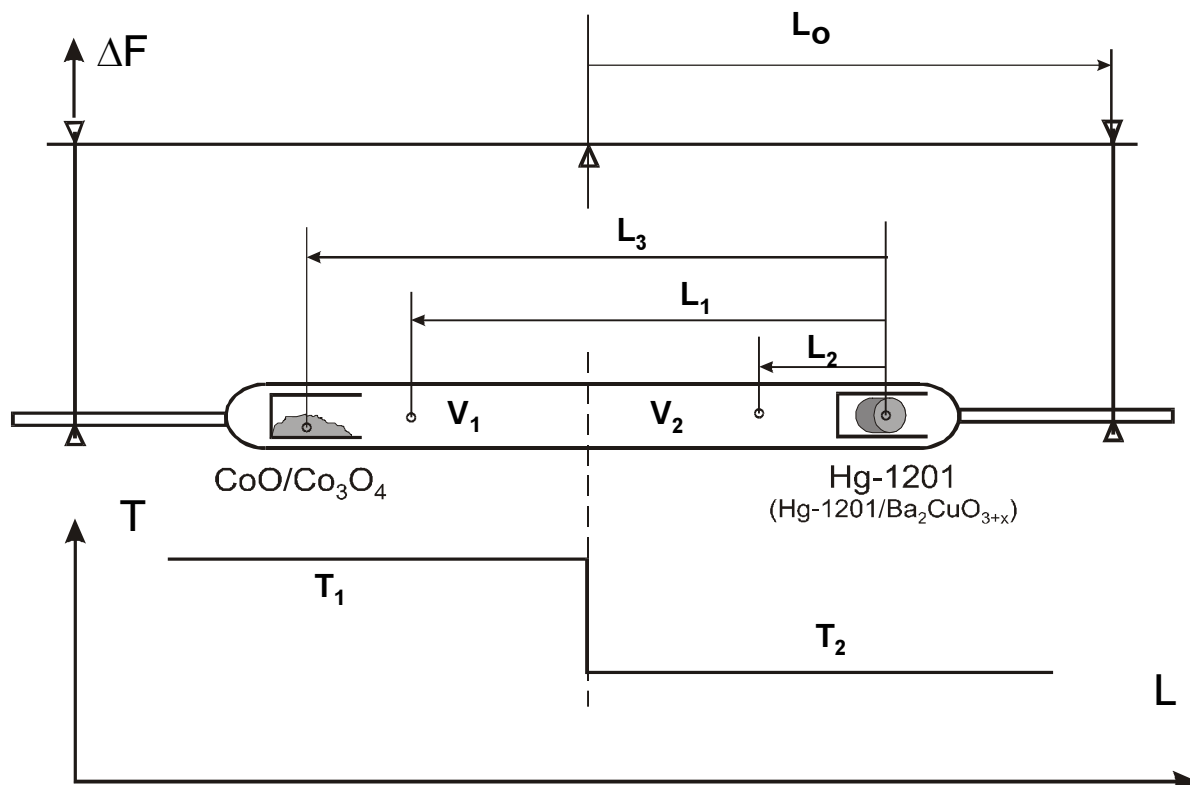


Fig.1.

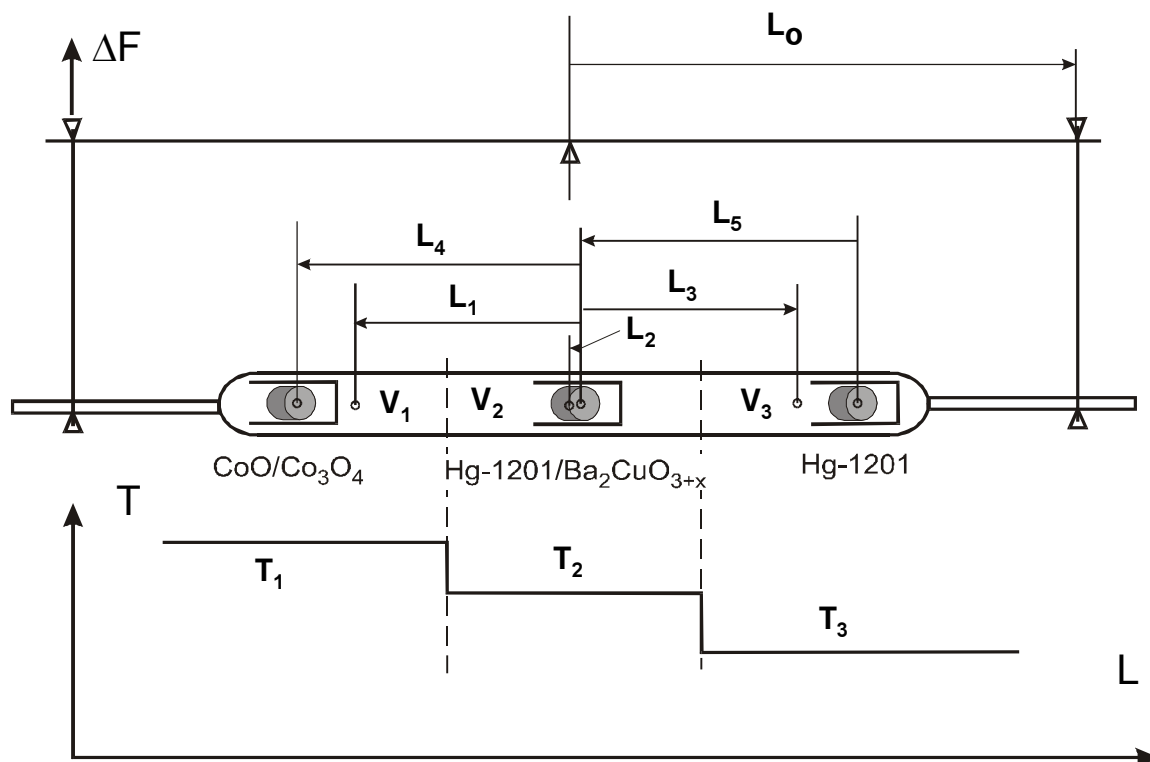


Fig.2.

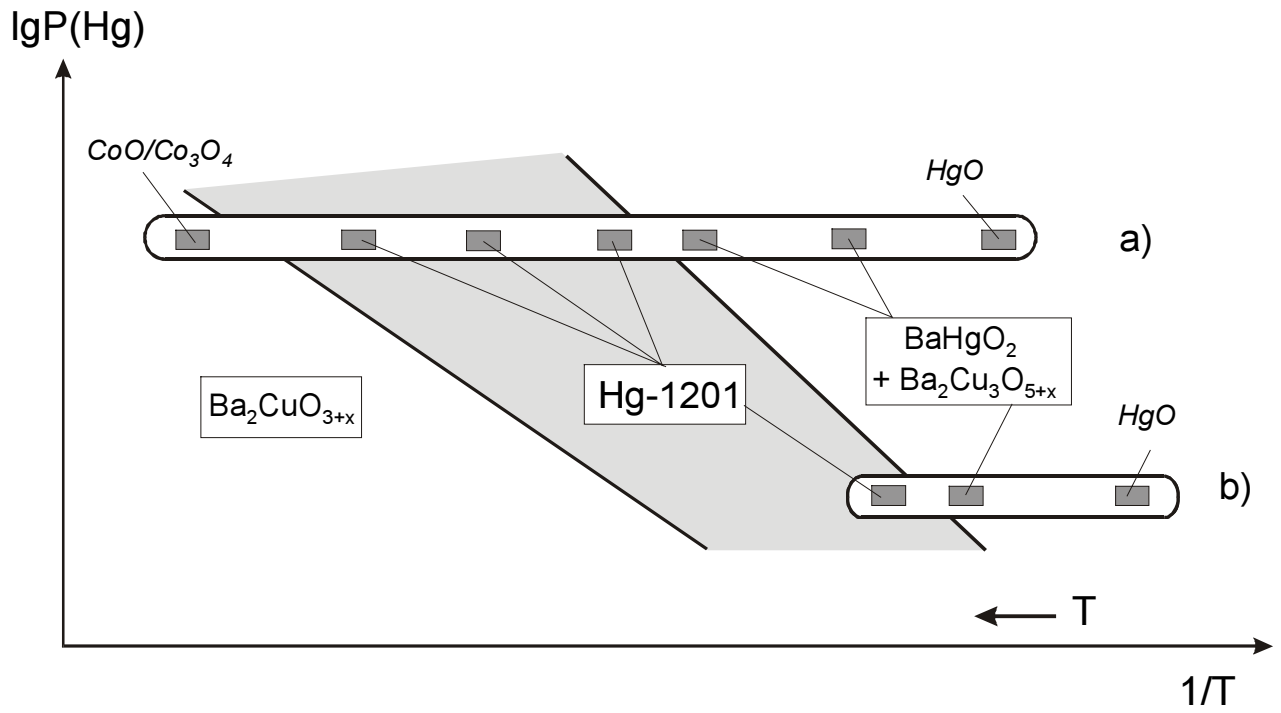


Fig.3.

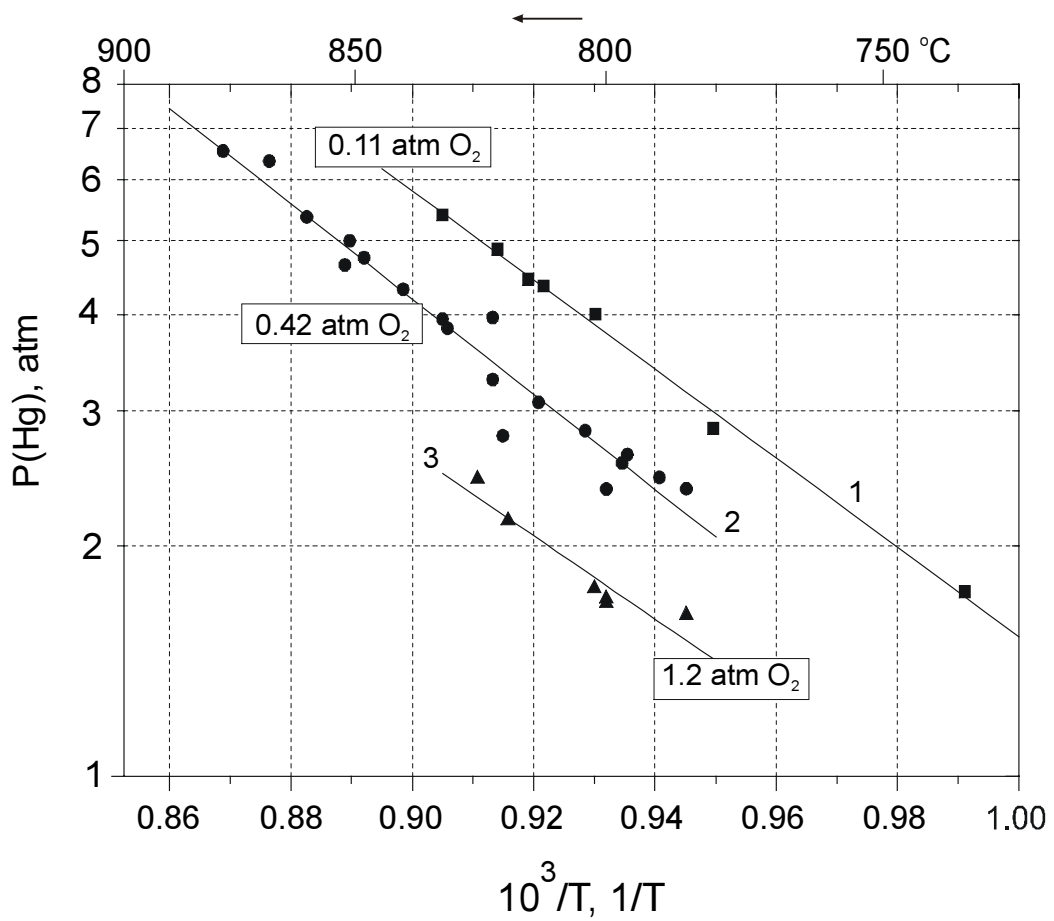


Fig.4.

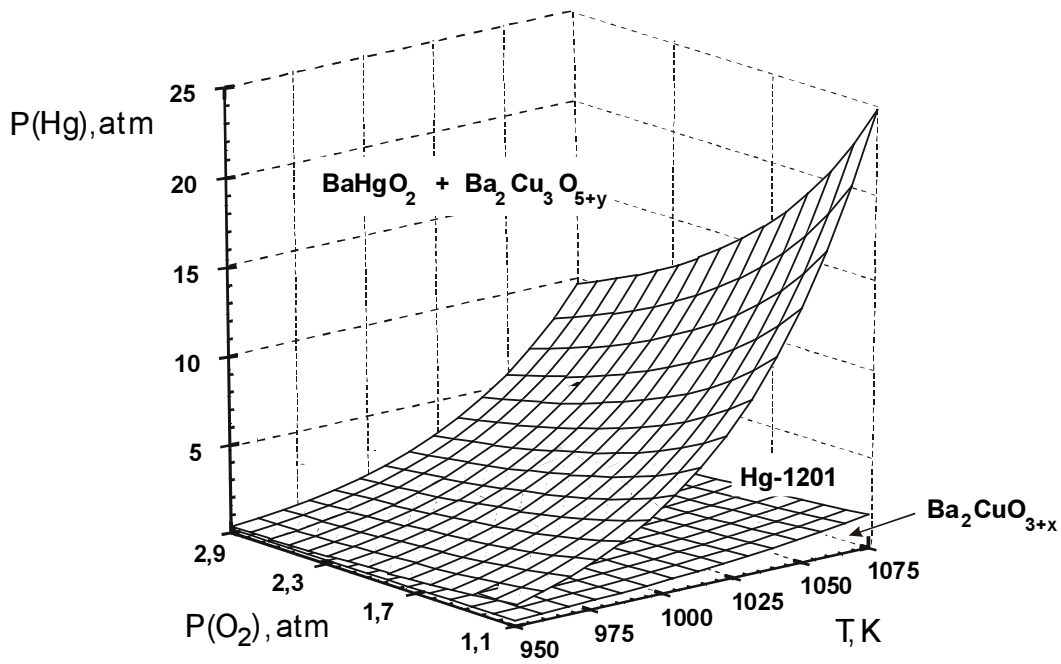


Fig.5.

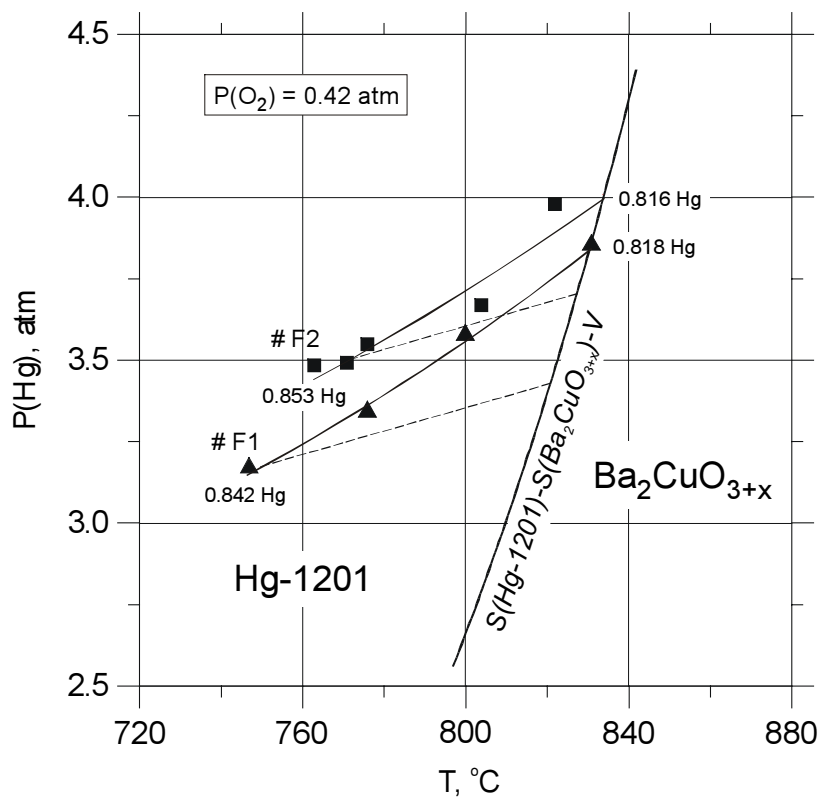


Fig.6.

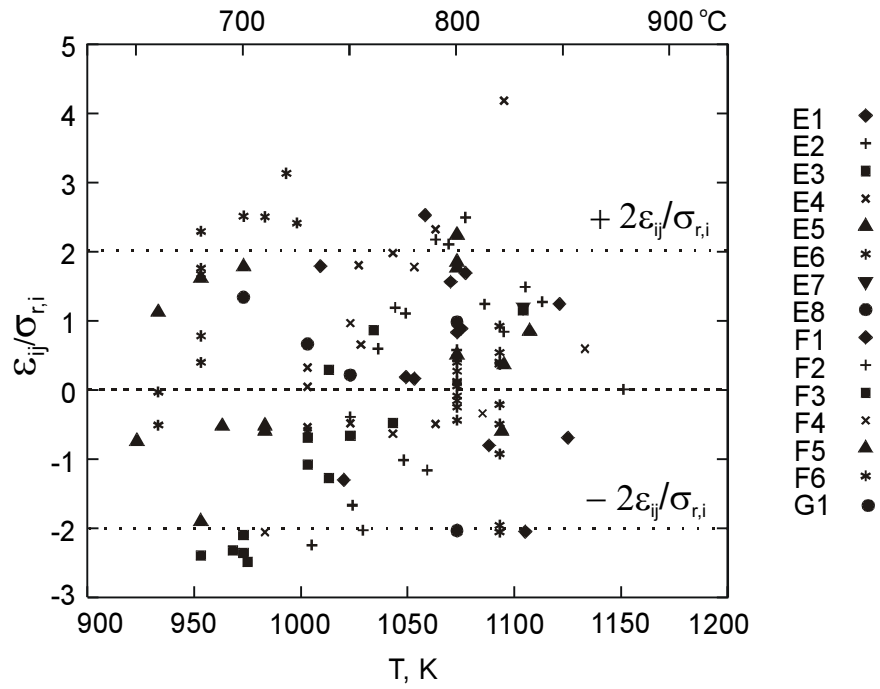


Fig. 7..

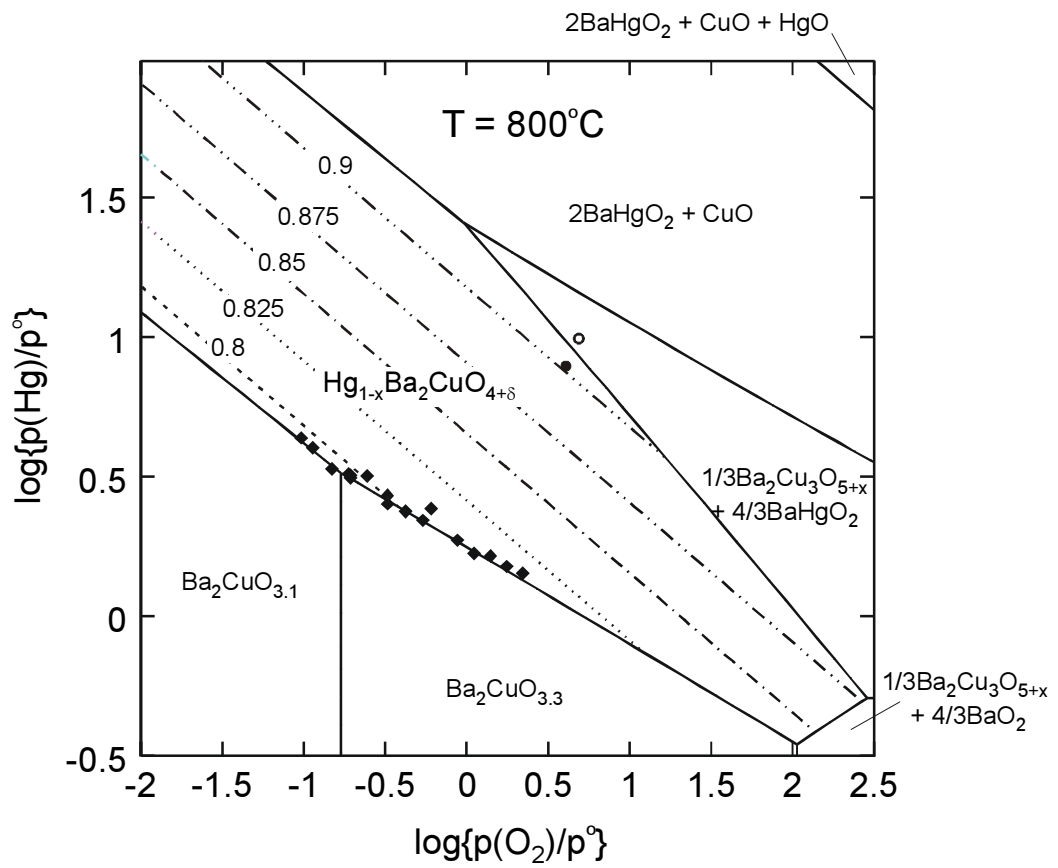


Fig. 8..

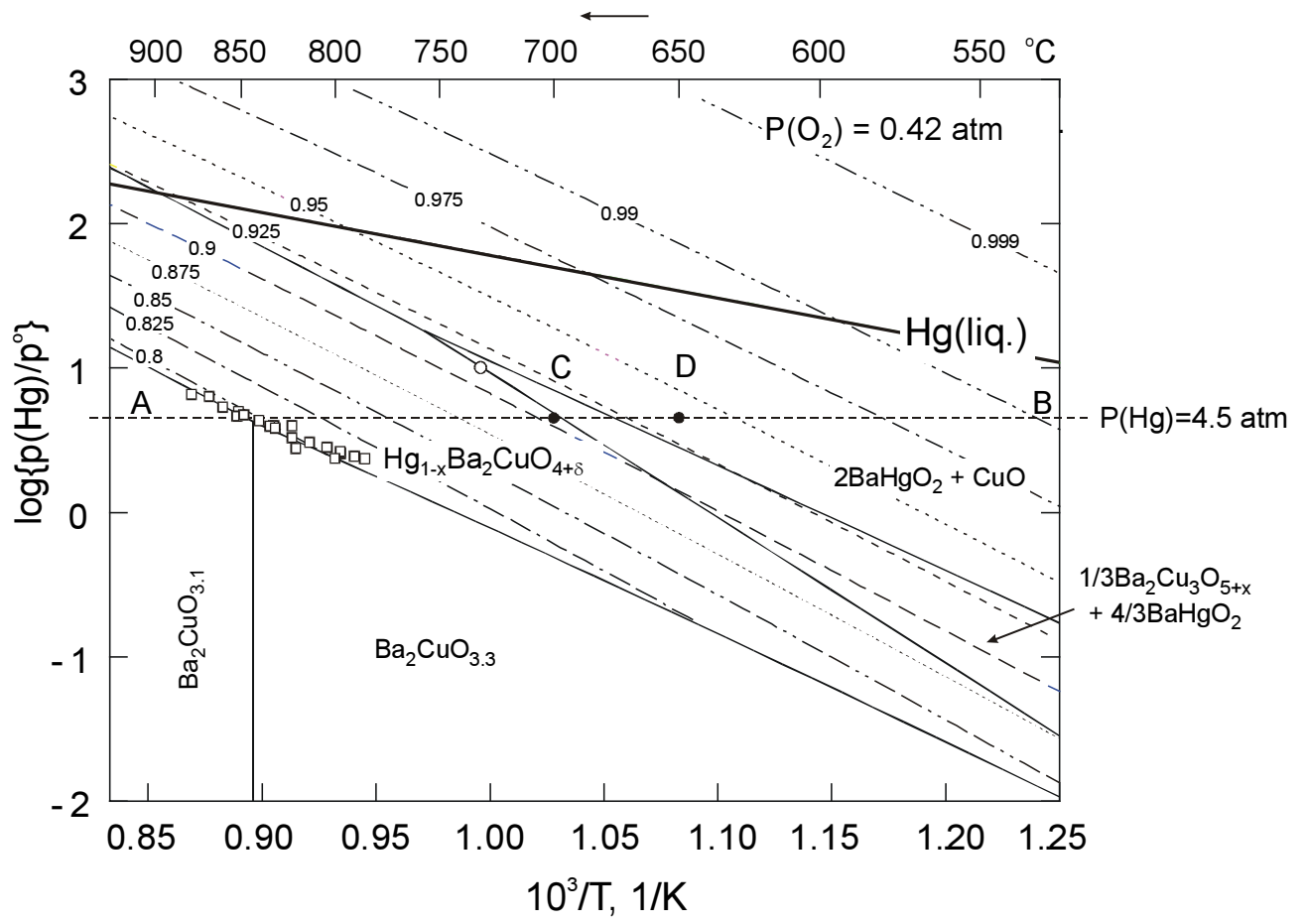


Fig. 9.